JOURNAL OF APPLIED ELECTROCHEMISTRY **29** (1999) 293–299.

Nickel ferrite as inert anodes in aluminium electrolysis: Part I Material fabrication and preliminary testing

E. OLSEN[1]* and J. THONSTAD[2]

[1]*SINTEF Materials Technology, N-7034 Trondheim, Norway;* [2]*Department of Electrochemistry, Norwegian University of Science and Technology, Norway*
*(*author for correspondence, e-mail: espen.olsen@matek.sinef.no)*

Received 23 May 1997

Dense, sintered samples of nickel ferrite/nickel oxide–copper cermets were produced and characterized. Three compositions were chosen, each with different NiO content. A new method of powder preparation involving no use of water as dispersant resulted in a well-dispersed ceramic phase with smaller metal grains than previously reported. The individual phases in the cermets were analysed quantitatively using energy-dispersive X-ray microanalysis, and significant differences between the materials were found. The electrical conductivity of the materials was measured, showing interesting properties not previously described. Reaction sintering was tried and found to lead to a microstructure different from that obtained with pre-calcined powder. The nickel contamination level in the electrolyte did not reach steady state after 4 h of electrolysis. Iron and copper did seem to reach steady state after some irregular behaviour early in the tests. The total contamination level of anode constituents in the deposited metal was as low as 0.116 wt%. These encouraging results seemed to be partly related to the cell configuration giving very slow mass transfer from the electrolyte into the metal.

Keywords: *aluminium*, *cermet*, *electrode*, *electrolysis*, *inert*, *$NiFe_2O_4$*

1. Introduction

As long as the Hall–Heroult process for aluminium production has been operating, the search for an inert anode material has been an issue in pursuit of new technology. In the present process, consumable carbon anodes are used, the anode product being CO_2. With an inert anode, the cell reaction will be,

$$Al_2O_3 = 2\,Al + \tfrac{3}{2}O_2 \qquad (1)$$

The basic requirements for an inert anode are: (i) exhibit a low corrosion rate, (ii) be a good electronic conductor, (iii) not to contaminate the produced metal to any significant degree, (iv) be thermally stable up to electrolysis temperature as well as exhibit adequate resistance to thermal shock and (v) be economically feasible. No material has yet been found which meets all these requirements.

As far back as the 1930's Belyaev and Studentsov [13, 14] examined candidate materials for inert anodes and focused on various oxides and ferrites with low solubilities in cryolitic melts. No firm conclusions were drawn, but a number of materials were found to have very low solubilities in molten cryolite. More recently, Aluminum Company of America (Alcoa) conducted, with support by US Department of Energy, a significant work on the use of ferrites [1]. Their effort ended in 1986, having arrived at a new cermet material consisting of a nickel ferrite–nickel oxide ceramic containing copper as a metal phase to provide acceptable electrical conductivity combined with good corrosion resistance. The ceramic matrix contained 18% (wt% when not otherwise stated) excess NiO to assure an activity coefficient of 1 for nickel oxide, as this phase has a significantly lower solubility in cryolite than Fe_2O_3 [1]. Battelle-Pacific Northwest Laboratories continued this work, but were not able to reproduce the best results obtained by Alcoa with their original composition [2–6]. More recently a review of new materials for the use in aluminium production with an emphasis on electrode materials has been published [12]. A more complete review of pertinent literature will be given in Part II of this paper.

In the present study we have used the Alcoa material as a basis and taken a new approach by applying different manufacturing methods to achieve a more fine-grained structure of the $NiFe_2O_4$ cermets, and have performed screening tests over 4 h to evaluate the performance of anodes with varying proportions of excess NiO. A point was made to study the dissolution of anode constituents from the cermet into the melt as a function of the amount of excess NiO in the ceramic phase of the anodes. In the cell used, steady-state impurity levels in the electrolyte were reached after a period of only 10 min depending somewhat on the species in question. The contamination of anode constituents in the cathode metal was

also studied, and the anode corrosion rate was determined. The used anodes were cut and the active surface of the anodes was studied by SEM to evaluate the material behaviour.

2. Objectives

In this work we wanted to use alternative methods for producing ceramic powders to see if materials with better characteristics could be obtained. In the final composition studied by Alcoa, excess NiO was added to the ceramic phase of the cermets. The reason for this was that of the two individual oxides, Fe_2O_3 and NiO, forming $NiFe_2O_4$, the latter has the lowest solubility in the electrolyte. We wanted to study the effect of the addition of NiO, both on the performance in electrolysis tests, and on the properties of the sintered cermet samples.

3. Material fabrication

3.1. *Experimental*

The powders were prepared from commercial grade chemicals. The suppliers and specifications (purity, grain size etc.) were: Fe_2O_3: Harcros pigments, USA, low silica type, Pigment grade, 99.3%, 5 μm. NiO: Novamet, USA, high purity green NiO, 99.98%, 5 μm. Ni: Aremco Products, USA, electronic grade, 99.9%, 3 μm. Cu: Aremco Products, USA, 99.8%, 1–5 μm.

Powders corresponding to 1200 g of a Fe_2O_3–NiO mixture of the desired composition were dispersed in 1000 ml n-hexane (Merck, pa.) using 10 g fish oil (NMD) as dispersant and mixed for 18 h in a stainless steel ball mill. An organic solvent and dispersant were used rather than water because water may cause oxidation of the metal particles. The mixture was dried and calcined at 1000 °C in air for 2 h to form the ferrite phase. Metal powders (Cu + Ni) were added to the calcined powder, and the mixture was again transferred to the ball mill and milled in a similar dispersion for an additional 18 h before drying and screening through a 60 mesh screen. No binder was added to the powder, as the metal present in the powder was considered to be sufficiently ductile to produce dense, machinable green bodies. Three different compositions were prepared, with 0 wt% excess NiO, 17 wt% excess NiO and 23 wt% excess NiO in the ceramic phase respectively. The metal phase was modified compared to Alcoa's original composition by adding 3 wt% Ni to the metal powder already constituting 17 wt% Cu, making it altogether 20 wt% metal phase. Nickel has better wetting characteristics than copper towards the oxide phases [1], so adding Ni should lead to smaller metal grains in the sintered samples. The physical properties of the sintered samples are listed in Table 1, and the compositions of the individual phases in the materials after sintering are listed in Table 2. The Fe/Ni molar ratio in stoichiometric $NiFe_2O_4$ is 2.

The powders were vibratory pre-compacted in latex moulds which were sealed and transferred to a cold isostatic press (CIP). The CIP pressure was 300 MPa. The green body density was about 60% of theoretical. The sintering was conducted in a closed tubular furnace. The maximum sintering temperature was 1350 °C in Ar atmosphere. The same overall sintering cycle as described by Weyand was used [3]. The sintered samples had a strong metallic lustre with a few scattered metal protrusions on the surface, indicating that the metal content was close to what could be contained without excessive metal bleed-out. Samples were prepared for characterization by SEM and X-ray diffraction (XRD). XRD showed no traces of uncalcined powder or foreign phases.

Reaction sintering where the calcination process takes place during the final sintering cycle was also tried. The powders were prepared by mixing the NiO, Fe_2O_3 and Cu/Ni powders in one step with subsequent sintering, according to the procedure described above.

3.2. *Electrical conductivity measurements*

The electrical conductivity versus temperature was measured with a standard dc four-point technique. A special device was constructed, continuously monitoring the dc current and voltages as shown in Fig. 1. The parameters were logged with a computer-based logging system every 10 s. The sample was placed in a closed furnace and heated from room temperature to 1000 °C in air.

3.3. *Material characterization*

In Tables 1 and 2 the compositions and some properties of the materials are listed. Relative atom% re-

Table 1. Properties of sintered samples of different compositions

% *excess NiO*	*Height* /mm	*Diameter* /mm	*Weight* /g	*Density* /g cm^{-3}	*TD* /g cm^{-3}	% *of TD*
0	50.2	25.4	126.50	5.06	5.82	86.9
17 (a)	46.7	23.9	127.00	6.06	6.18	98.1
17 (b)	49.4	24.9	139.03	6.12	6.18	99.0
17 (Rx)	16.0	8.61	10.70	6.18	6.18	100
23	46.5	24.1	129.21	6.32	6.52	96.9

For 17 wt% excess NiO, sample (a) was prepared from powder produced as described above and (b) was prepared from a different batch of powder, but otherwise as (a). (Rx) is reaction sintered material (see text). TD is theoretical density.

Table 2. Composition of the individual phases in the sintered materials as determined by X-ray microanalysis (XRMA)

Excess wt% NiO in material	*Individual phase*	*Fe* /rel. at%	*Ni* /rel. at%	*Cu* /rel. at%
0	Metal	5.4 ± 0.2	37.1 ± 0.7	57.6 ± 0.9
	$NiFe_2O_4$	77.1 ± 0.6	22.0 ± 0.5	0.8 ± 0.3
17	Metal	4.1 ± 0.2	40.3 ± 0.6	55.3 ± 0.8
	NiO	24.6 ± 0.3	75.3 ± 0.7	0
	$NiFe_2O_4$	75.0 ± 0.5	25.0 ± 0.5	0
23	Metal	4.4 ± 0.2	32.6 ± 0.6	62.7 ± 0.9
	NiO	16.7 ± 0.3	82.3 ± 0.8	0
	$NiFe_2O_4$	71.0 ± 0.6	27.3 ± 0.5	1.0 ± 0.3

lates to the analytical data collected from the energy spectra in the X-ray microanalyser (XRMA) of the SEM. A Be window was used which did not allow analysis of light elements such as oxygen. Battelle-PNL [7] found the Fe/Ni atomic ratio to be in the range 2.2–2.6 in the ferrite phase and 0.09–0.2 in the NiO phase. For NiO, this is consistent with the ratio found in this work, but not for the Fe/Ni ratio in the ferrite, which in Table 2 ranges 2.6–3.5. This implies that the ferrite phase in this work had a higher degree of non-stoichiometry than the materials used by Battelle-PNL; this is most likely because Fe^{2+} cations substituted Ni^{2+} in the spinel lattice.

The metal phase seemed to be of approximately equal composition in all the materials (Table 2). There was, however, a remarkably high Ni content in the metal phase. The added powders (17 wt% Cu and 3 wt% Ni) should give a content of 15 wt% Ni in the metal phase, as also reported by Alcoa [7]. In their work Ni powder was not added, the Ni content being the result of an exchange reaction (2) between Cu, $NiFe_2O_4$ and NiO,

$$\begin{aligned} &Cu + NiFe_2O_4 + NiO \\ &\quad = Cu_xNi_{1-x} + Ni(II)_yFe(II)_{1-y}Fe(III)_2O_4 \\ &\qquad + Ni(II)_zFe(II)_{1-z}O \end{aligned} \tag{2}$$

Addition of Ni powder to the metal prior to sintering was believed to fix the Ni activity in the alloy at equilibrium from the beginning, suppressing the exchange reaction (2). This did not seem to be the case, as we found the Ni content in the metal phase in the anodes prepared in this work to be about 30 wt% (Table 2). A possible explanation for the high Ni content in the metal phase could be carbothermic reduction of the oxide phases by carbon residues of the organic solvent and the dispersant. This is a general problem when processing ceramic powders in organic solvents. Alcoa [1] processed the powders in water which, on the other hand, can lead to oxidation of the surfaces of the metal particles and, subsequently, different sintering characteristics and grain structure. It was not possible to disperse the powders satisfactorily without adding the dispersant.

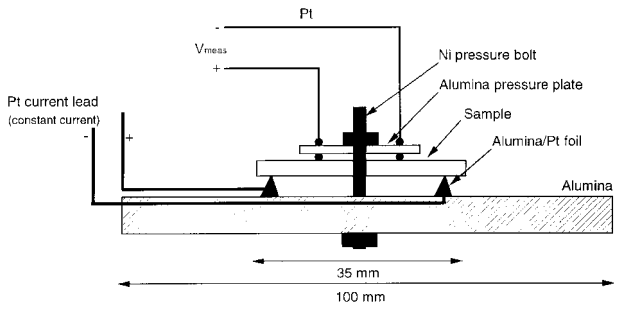

Fig. 1. Device for measurement of electrical conductivity at high temperatures.

SEM micrographs of polished samples of the sintered materials are shown in Fig. 2. There are no visible differences between the samples except for higher porosity in the material with no excess NiO (Fig. 2(a)). The reaction sintered material had a different microstructure compared to the material made with pre-calcined powder. The structure is shown in Fig. 2(d). The metal grains are not spherical and seem to have preferred orientation in certain regions of the material. This material was also very dense, the measured density being close to theoretical.

3.4. *Conductivity measurements*

The electrical conductivity as a function of temperature for the materials with excess NiO content investigated in this work is shown in Fig. 3. The conductivity was definitely of semiconducting nature. A striking feature was the behaviour at ~1000 °C where a phase transition apparently occurred. This has not been described in earlier literature. Weyand measured the conductivity of a similar material up to 1100 °C but did not observe this change in conductivity [7]. Ray [8] investigated a material containing no metal phase but otherwise of similar composition, and neither in that case was such behaviour observed. The materials used in this work have not been reported to undergo any transitions at this temperature, and the melting point of the metal phase is above 1100 °C [9]. It is interesting to note conductivity increases in the material with higher content of NiO. A number of specimens of each composition were tested and the reproducibility of the results was good.

The conductivity of the material with pure nickel ferrite as ceramic phase exhibited a totally different behaviour compared to the material with excess NiO. The conductivity vs. temperature is shown in Fig. 4. In the low temperature range below ~600 °C, the conductivity was significantly lower than for the NiO-rich material, but still of semiconducting nature, rising with the temperature. A remarkable change took place at 650 °C on the cycle of rising temperature. The conductivity jumped from a mere $20\,S\,cm^{-1}$ to $275\,S\,cm^{-1}$. It was no longer semiconducting, but exhibited a strong metallic-like behaviour as it gradually decreased with increasing temperature to $30\,S\,cm^{-1}$ at 1000 °C. On the reverse cycle a strong degree of hysteresis was observed as the semiconducting region was

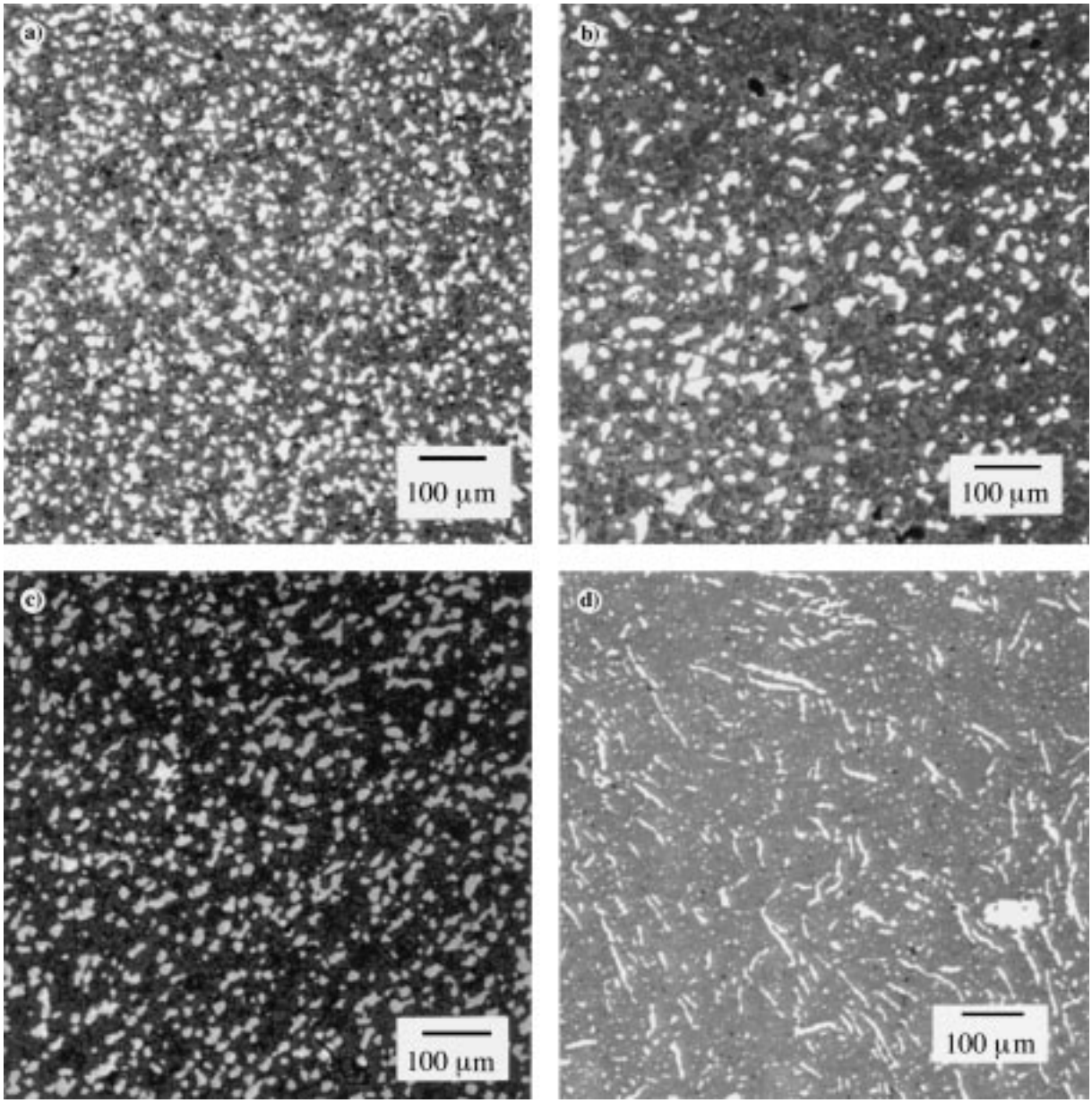

Fig. 2. The different materials investigated in this study: (a) no excess NiO; (b) 17 wt% excess NiO; (c) 23 wt% excess NiO; and (d) reaction sintered material with 17 wt% excess NiO.

not fully reestablished until 580 °C. The transition started at the same temperature as on the ascending cycle, but was not as abrupt. This behaviour, which was confirmed by repeated experiments, might be related to the ceramic phase, as the metal phase was practically the same as in the other cermets. Literature data show a phase transition in nickel ferrite at 600 °C as indicated by a discontinuity in C_v [10]. Thermal expansion data for this material have not been reported in the literature. The order of the phase transition remains to be determined.

4. Electrolysis tests

4.1. *Experimental set-up*

In the short-term tests the electrochemical cell shown schematically in Fig. 5 consisted of a graphite crucible lined with a cylindrical alumina sleeve. The inner diameter was 65 mm. The cathode consisted of a rectangular plate of TiB_2–graphite composite (95 wt% TiB_2 + 5 wt% C, Great Lakes Carbon, USA). This plate was fastened to the graphite crucible with carbon cement. The cathode area was 10 cm^2, and alumina cement (Thermomax) was cast as insulation around the cathode. The crucible was polarized cathodically via an Inconel rod. The cell is shown schematically in Fig. 5. The temperature was 960 ± 2 °C which was monitored during the experiment using a Pt/Pt + 10% Rh thermocouple in a sintered alumina sleeve immersed in the electrolyte. Also immersed in the electrolyte was an Al/W reference electrode.

The electrolyte was prepared from technical grade natural Greenland cryolite, sublimed AlF_3, reagent grade CaF_2 and technical grade alumina, and had the composition: 10 wt% CaF_2, 11 wt% AlF_3, 8 wt% Al_2O_3, balance cryolite.

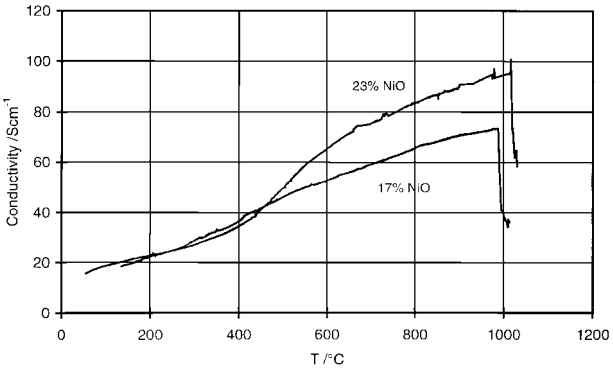

Fig. 3. Electrical conductivity versus temperature for the cermet materials containing excess NiO.

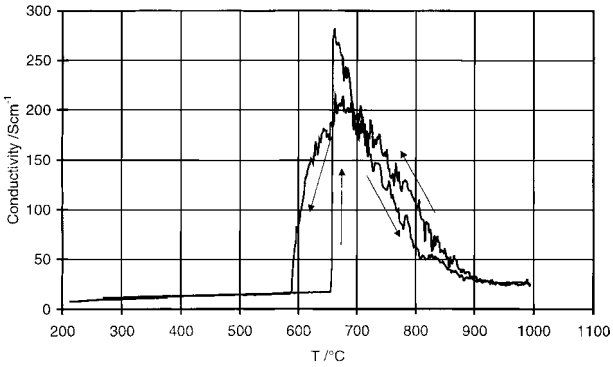

Fig. 4. Electrical conductivity versus temperature for the cermet material without excess NiO in the ceramic phase.

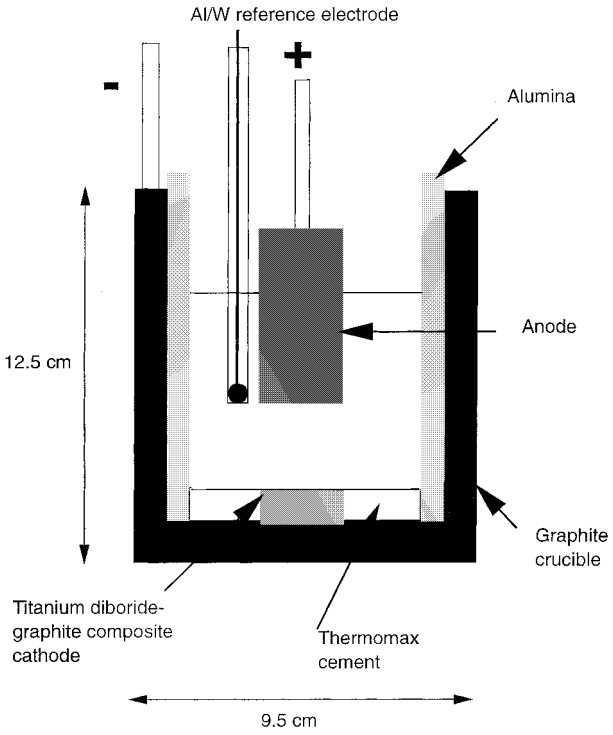

Fig. 5. Electrochemical cell used in the tests.

The crucible contained a total of 420 g electrolyte. During electrolysis Al_2O_3 was added every 30 min in amounts based on the electrolytic consumption rate at 70% cathodic current efficiency. An open, cylindrical furnace was used. Aluminium was not added prior to electrolysis.

Electrolysis was run for 4 h. The anode diameter was 2.5 cm, which, with an immersion depth of 3 cm, gave approximately 25 cm^2 active, polarized surface area. The anodic current was 25 A, giving an overall current density of 1 A cm^{-2}. The cathodic current density was 2.5 A cm^{-2} in the beginning of the experiments. The active cathode surface area changed somewhat during the experiments due to the deposition of Al, which eventually formed a semisphere on the wettable cathode.

The cell and reference voltages were measured with a computer-based logging program. After electrolysis the anode was raised out of the melt while maintaining polarization so as to prevent reduction of the anode material by dissolved metal. The cell was left to cool with the anode resting above the electrolyte. After cool-down the anode assembly was removed and the cathode with its metal semisphere was removed from the crucible for analysis. No visible corrosion was observed on the anodes after electrolysis. The corrosion rates had to be determined from the contamination of the metal and the electrolyte.

Samples of the electrolyte were taken before immersion of the anode and every 5 min during the first 30 min of electrolysis. After this initial period, samples were taken less frequently associated with addition of Al_2O_3. The samples were frozen on a graphite rod which was quickly dipped into the electrolyte and removed for solidification. Each sample weighed approximately 1.5 g. The samples were ground in an agate mortar and analysed with X-ray fluorescense spectroscopy (XRF). The precision of the analyses was approximately 5% of the measured quantity. Metal samples were cut from the cathodically deposited metal semisphere and dissolved in concentrated HCl to be analysed by atomic absorption (AA). The precision of these analyses was about 10% for measured values below 100 ppm, 5% for values between 100 and 1000 ppm and 3% above 1000 ppm.

4.2. *Results and discussion; electrolysis tests*

As mentioned above, during the first 30 min of electrolysis, electrolyte samples were taken at 5-min intervals to study the dissolution process of the anode material. Subsequently, electrolyte samples were taken every half hour just before addition of alumina. The samples were analysed for the content of anode components, and a typical set of results is plotted in Fig. 6.

The present data were taken over a time-span of 4 h. It can be disputed whether steady state was reached. It is, however, clear that the different cermet compositions showed a varying degree of dissolution of the anode components. The iron concentration rose rapidly for all compositions from a background level of 200–250 ppm and remained steady at 300 ppm. This is a dynamic value as Fe species dis-

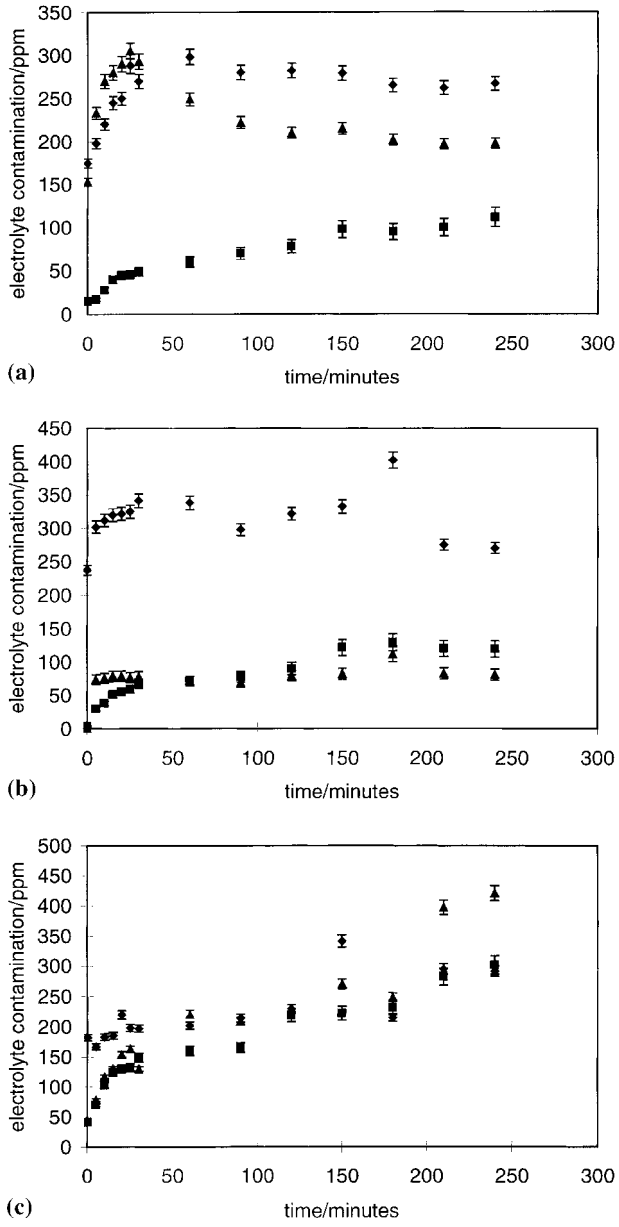

Fig. 6. Elemental analyses of the electrolyte contamination of anode constituents versus time for the cermet electrodes: (a) no excess NiO; (b) 17 wt% excess NiO; (c) 23 wt% excess NiO in the ceramic phase of the anode materials. (◆) Fe; (■) Ni, (▲) Cu.

solve at the anode surface and are reduced into the metal pad according to Reaction 3,

$$Al + \tfrac{3}{n}M^{n+} = Al^{3+} + \tfrac{3}{n}M \qquad (3)$$

In addition, some Fe entered the electrolyte with the added alumina which contained 110 ppm Fe_2O_3. The anode material containing 17 wt% excess NiO, which was identical to the Alcoa composition, would be expected to yield results similar to those obtained by Alcoa [7]. The Fe contamination is somewhat lower in the present data (300 vs 400 ppm). Iron is, however, a questionable element to use for comparison, as Fe impurities were present in significant amounts in all parts of the cell as well as in the alumina being fed to the electrolyte. Compared to the solubility data published by DeYoung [11] who found the solubility of Fe and Ni from $NiFe_2O_4$ pellets to be 580 and 90 ppm respectively, the results from this study are lower by a factor of about 2. The conditions were approximately the same in the two studies, and this may indicate that the melt was not saturated with respect to the two elements. This will be further elaborated in Part II (long-term testing) of this paper.

For Cu and Ni also the results vary for the different compositions studied. In both materials containing excess NiO, the NiO activity should be unity and the concentration might be expected to be roughly the same for all elements, possibly adjusted for the somewhat higher relative content of nickel. In the long run it might be expected that the corrosion rates reflect the relative contents of the various elements in the anode material. From Fig. 6(b) and (c) it is seen that this assumption holds for Fe and Ni. The values for Cu are, however, higher than expected if the dissolution should reflect the relative contents in the material. This might be due to metal nodules being formed on the anode surface during sintering. Care was taken to remove these before testing, but some might have escaped the machining after sintering.

The contamination of anode constituents in the metal after the tests is listed in Table 3. The values differ rather strongly between the materials, but the material with no excess NiO in the ceramic phase has the lowest total contamination, indicating that this material exhibited the lowest corrosion rate. It is difficult to draw firm conclusions or give actual corrosion rates based on these results as the anodes were electrolysed for only 4 h. This was not considered enough to reach steady state for anode constituents entering the metal, especially not in the case of Fe, which also entered the electrolyte from other sources. This topic will be discussed in Part II of this paper.

The relative electrolyte concentration of Fe and Ni in this experiment might be expected to reflect the composition in Table 2, but this is not the case. The present study shows a Fe/Ni weight ratio in the melt of roughly 3 after 4 h of electrolysis, which corresponds to a Fe_2O_3/NiO ratio of 3.35 (see Figs 6(a)–(c). In the anode material this ratio is 2.05, indicating non-stoichiometric dissolution of the oxide phase. In the deposited aluminium the Fe/Ni ratio was 4.68 for the all-ferrite material (Table 3). These variable data may also be due to Fe contamination from other sources, such as the crucible material, the crucible lining and the added alumina. In the anode material the weight ratios of Fe_2O_3/Cu and NiO/Cu are 2.72 and 1.28, respectively.

Table 3. Metal contamination of anode constituents

Excess wt% NiO in the material	*Fe* /ppm	*Ni* /ppm	*Cu* /ppm
0	838.3	178.8	152.3
17	1129.5	89.6	207.9
23	1621.2	451.5	517.0

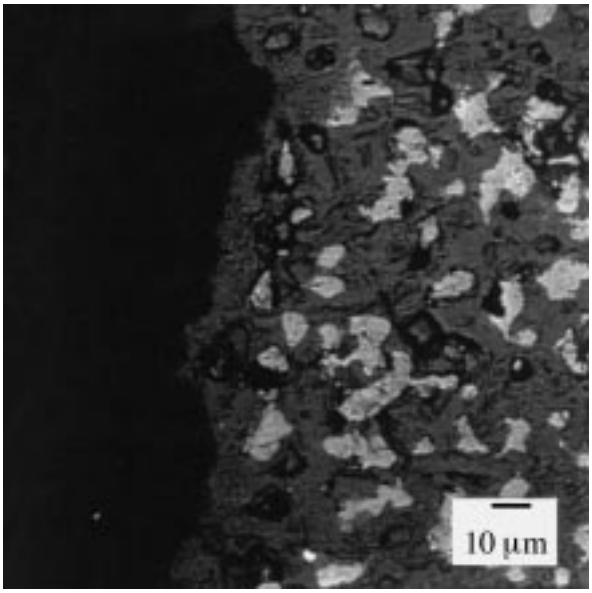

Fig. 7. SEM micrograph of a cross-section of an anode with 0 wt% excess NiO in the ceramic phase showing the anode surface layer.

For all three materials tested, the values for the Fe concentration in the electrolyte seemed to reach a stable value close to 300 ppm after 30 min. For the other components a true steady state did not seem to reach during the duration of the experiments. Initially, the Ni level rose quickly, and after 30 min of electrolysis the curve levelled off, but continued to rise at a lower rate. Cu seemed to follow the same pattern for the compositions containing excess NiO. For the material with no excess NiO (Fig. 6(a)), the Cu level rose sharply to a high level and subsequently decreased. All these observations led to the conclusion that longer tests were needed to determine the steady-state values of Ni and Cu contamination with these cermet electrodes, as will be shown in Part II.

The electrolysis tests indicated that the material corroded in a controlled manner. Once the initial dissolution of the metal grains directly exposed to the electrolyte had occurred, a semistable all-oxide outer layer was formed which seemed to dissolve slowly, inhibiting selective dissolution of the underlying metallic grains. This layer was measured with SEM to be of about 20 μm thickness for all the three compositions tested. A SEM picture of the anode surface after electrolysis is shown in Fig. 7. The total contamination level of anode constituents in the deposited metal was as low as 0.116 wt%. A reason for the low transfer of contaminating species into the metal might be related to the cell configuration used. In a cell with horizontal electrodes, the convection pattern might give rise to a stagnant layer above the cathode which will slow down mass transfer from the electrolyte into the metal. This will also be further discussed in Part II. Attempts to use a vertical electrode configuration were abandoned because of uneven current distribution caused by the low electrical conductivity of the anode material, as well as failure to collect the produced metal in a confined space.

Acknowledgements

The authors gratefully acknowledge financial support from the Norwegian aluminium industry and the Norwegian Research Council. This work was conducted in partial fulfilment of the requirements for a dr.ing. (Ph.D.) degree by one of the authors (E.O.).

References

[1] J. D. Weyand, D. H. DeYoung, S. P. Ray, G. P. Tarcy and F. W. Baker, 'Inert Anodes for Aluminium Smelting, Final Report', (Aluminium Company of America, Alcoa Laboratories, Alcoa Center, 1986), DOE No. DOE/CS/40158-20, Department of Energy, Idaho Operations Office, Idaho Falls, ID (1986).

[2] C. F. Windisch and S. C. Marschman, 'Electrochemical Polarization Studies on Cu and Cu-containing Cermet Anodes for the Aluminium Industry', Battelle-PNL report No. PNL-SA-14299, Pacific Northwest Laboratories, Richland, WA, USA (1986).

[3] C. F. Windisch, *J. Electrochem. Soc.* **138** (1991) 2027.

[4] C. F. Windisch and N. D. Stice, 'Report on the Source of the Electrochemical Impedance on Cermet Inert Anodes', Battelle-PNL report No. PNL-7629, Pacific Northwest Laboratories, Richland, WA, USA (1991).

[5] C. F. Windisch and N. D. Stice, 'Final Report on the Characterization of the Film on Inert Anodes', Pacific Northwest Laboratory, Richland, WA, USA (1991).

[6] C. F. Windisch, 'Comparative Study on Cermet and Platinum Anodes for the Electrolytic Production of Aluminium', Electrochemistry in Mineral and Metal Processing III, The Electrochemical Soc., Pennington, NJ (1992).

[7] J. D. Weyand, 'Manufacturing Process Used for the Production of Inert Anodes', Light Metals 1986, The Minerals, Metals and Materials Soc., Warrendale, PA (1986) pp. 321–339.

[8] S. P. Ray, 'Inert Anodes for Hall Cells', Light Metals 1986, The Minerals, Metals and Materials Soc., Warrendale, PA (1986) pp. 287–298.

[9] 'Binary Alloy Phase Diagrams', vol. 2, 2nd edn, ASM International, USA (1990).

[10] Y. S. Touloukian, 'Thermophysical Properties of High Temperature Solid Materials', vol. 4b, Collier-Macmillan ltd., London, UK (1967) p. 1089

[11] J. D. DeYoung, *in* 'Conference paper, Light Metals 1986', (edited by R.E. Miller). The Minerals Metals and Materials Soc., Warrendale, PA (1986) pp. 209–309.

[12] H. Zhang, V. De Nora and J. A. Sekhar, 'Materials Used in the Hall-Heroult Cell for Aluminium Production', The Minerals Metals and Materials Soc., Warrendale, PA (1994).

[13] A. I. Belyaev and A. E. Studentsov, *Legkie Metally* **6**(3) (1937) 17.

[14] A. I. Belyaev and A. E. Studentsov, *Legkie Metally* **8**(1) (1938) 7.